Engineering and Technology Journal
Journal homepage: https://etj.uotechnology.edu.iq

Impact of laser energy on the synthesis and antibacterial performance of CdO nanomaterials

Ali A. Yousif[a], **Thikra A. Mejbel**[a*], **Kadhim A. Aadim**[b], **Wasan J. Kadhem**[c]

[a] Department of Physics, College of Education, Mustansiriyah University, Baghdad, Iraq.
[b] Department of Physics, College of Science, University of Baghdad, Jadriya, Baghdad, Iraq.
[c] Department of Scientific Basic Sciences, Faculty of Engineering Technology, Al-Balqa Applied University, Amman, Jordan.
*Corresponding author Email: thikramijbel@gmail.com

HIGHLIGHTS

- CdO nanoparticles synthesized by laser energies showed a cubic polycrystalline structure with nano-sized crystals.
- The bandgap decreased with rising laser energy: 2.6, 2.56 & 2.38 eV at 400, 500 & 600 mJ due to quantum effects.
- The nanoparticles showed antibacterial activity against S. aureus & E. coli, useful for effective agents.

Keywords:

Cadmium oxide nanoparticles; Pulsed laser ablation in liquid; Antibacterial activity; Optical properties; Nanoparticle synthesis.

ABSTRACT

The objective of the current work is to evaluate the antibacterial efficiency of cadmium oxide nanomaterials (CdO NPs) produced through pulsed laser ablation in liquid (PLAL) with laser energy ranging from 400 to 600 mJ. Several characterization techniques, including X-ray diffraction (XRD), UV-Vis spectroscopy, and atomic force microscopy (AFM), were harnessed to analyze synthesized CdO NPs. The nanoparticles had a spherical shape and a size distribution that reduced with higher laser energy. The XRD study confirmed a polycrystalline cubic structure, while AFM measurements disclosed a drop from 133 to 84 nm in the particle size as laser intensity rose. UV-Vis spectra revealed that intensified laser energy caused a narrowing of the bandgap, which was measured from 2.6 eV at 400 mJ to 2.38 eV at 600 mJ. CdO NPs' antibacterial activity has been determined against Staphylococcus aureus (SA) and Escherichia coli (EC) using the colony counting method. The results indicated a considerable reduction in bacterial colonies, with E. coli demonstrating more susceptibility than S. aureus. The findings indicate that PLAL-produced CdO NPs have high antibacterial characteristics, making them promising candidates for biomedical applications, particularly antibacterial coatings and therapies.

1. Introduction

Biomedical research is one of the many scientific fields that have witnessed a revolution as a result of nanotechnology, especially in the field of metal oxide nanoparticles (MO-NPs) [1]. By merging nanotechnology and biology, nanobiotechnology harnesses the unique characteristics of nanomaterials to interface with biological systems, facilitating the production of eco-friendly, biocompatible, and biogenic nanostructures [2]. Nanomaterials are used in a variety of biological applications, including fluorescent biological labeling [3], drug and gene delivery [4], pathogen identification via biomarkers [5], protein detection [6], DNA structural analysis [7], tissue engineering [8], tumor destruction through heating [9], purification and separation of biological material and cells, as well as MRI contrast enhancement [10], and phagokinetic investigations [11]. Among commercially available NPs, metal oxides such as silica (SiO_2), zinc oxide (ZnO), silver (Ag), tin oxide (SnO_2), titanium dioxide (TiO_2), and cadmium oxide (CdO) have acquired significant attention for their wide-spectrum applications in electronics, optics, and biomedicine due to their distinctive physicochemical features [12]. Interestingly, CdO NPs have manifested encouraging antibacterial characteristics, which has induced a significant focus on research due to the growing concern of antibiotic resistance, which could impart an inevitable threat to public health.

As a n-type semiconductor, CdO represents an inorganic compound with a faceted cubic crystal structure. With a density of 8,150 kg/m³, a refractive index of 2.75, and a bandgap that extends from 1.36 to 1.98 eV (indirect) and 2.2 to 2.5 eV (direct), CdO possesses a range of characteristics that make it appropriate for a variety of applications. It is an excellent material for application in photovoltaics, gas sensors, chemical catalysis, and other electronic devices due to its high carrier

http://doi.org/10.30684/etj.2025.158712.1929
Received 28 March 2025; Received in revised form 22 April 2025; Accepted 25 April 2025; Available online 29 April 2025
2412-0758/University of Technology-Iraq, Baghdad, Iraq

concentration, superior electrical conductivity, chemical stability, and optical transparency in the visible spectrum. Additionally, the material's clear transparency in the visible light range, combined with its excellent electrical conductivity, highlights its potential for a wide range of applications in optoelectronics and biomedical fields [2, 13-16].

With the wide spectrum of MO-NPs continuing to be harnessed in advance and recent biomedical research, CdO NPs have been explored as an attractive choice for versatile applications, especially in nanobiotechnology [17]. Several scenarios have been reported about the killing mechanisms of different nanoparticles, such as direct contact or ion release [18]. Some NPs can penetrate bacterial cell membranes and disrupt the metabolic processes owing to their tunable small size (1 to 100 nm). Besides, their ability to interface at the cellular level. Recently, it was reported in literature that CdO NPs, in particular, possess a strong antibacterial activity, that attributed to their dual ability to produce reactive oxygen species (ROS) and release Cd^{2+} ions. CdO was reported to be effective against a wide spectrum of infections, including strains that are well known to be resistant to antibiotics. This was attributed to its antimicrobial mechanisms as well as their unique size and shape of the nanoparticles, which interfere with bacterial functions. This particularly made CdO NPs an attractive candidate in the defense against drug-resistant bacterial infections, which are growing as a serious medical concern [2]. Several studies have investigated the antibacterial potential of CdO NPs. For instance, Hossain et al. [19], claimed a considerable anti-bactericidal activity posed by CdO NPs against gram-negative Escherichia coli (E. coli), while Shukla et al. [20], confirmed their antibacterial efficacy at varying doses on E. coli cells. Also, Ahmed et al. [21], further investigated CdO's antibacterial activity against a wide spectrum of harmful microorganisms the well-known diffusion method. Furthermore, Dixit, Bala, and colleagues have synthesized CdO and MnO NPs utilizing different methods, and claimed strong antibacterial, antioxidant, and antimicrobial activity [18]. Ismail et al. [22], developed CdO NPs harnessing green synthesis with Curcuma longa and showcased potent antibacterial efficacy against both Gram-positive and Gram-negative bacterial strains. Rhoda et al. [23], concluded that CdO and Cu-doped CdO nanoparticles were successfully synthesized using the co-precipitation method. Characterization techniques indicated their cubic structure, and both types exhibited significant antibacterial activity against Micrococcus luteus and Escherichia coli, with Cu-doped CdO showing enhanced efficacy. These nanoparticles hold promise as alternatives to conventional antibiotics due to their effectiveness against pathogenic bacteria. Fahad synthesised CdO NPs by PLA at different laser energies (200-500 mJ), which showed strong antibacterial and anti-biofilm activity against Staphylococcus aureus and E. coli. Higher laser energy produced smaller particles with enhanced inhibitory effects, indicating the potential of PLA for biomedical applications [24].

In this context, CdO NPs could be synthesized harnessing a wide variety of chemical and physical methods, such as chemical vapor deposition, sol-gel, and pulsed laser ablation in liquid (PLAL) [25,26]. In the meantime, typical chemical synthesis techniques were reported to be frequently utilizing dangerous chemicals that raise several environmental and safety issues. Meanwhile, green synthesis techniques, which use biological agents such as plant-derived phytochemicals and microbial enzymes, are a more claimed to be a more sustainable and environmentally friendly option [27]. However, the PLAL technique endows a clean and controlled method for nanoparticle production. This method eliminates the requirements for harmful chemical precursors, thus imparting a greener alternative for nanoparticle synthesis. PLAL technique has received distinguish attention amongst other physical production techniques due to the capability to avoid utilizing harmful chemicals. At the same time, it also bestows tunable properties via precise control over nanoparticle size, purity, and shape. This could be achieved through adjusting the fabrication parameters, such as laser energy during the PLAL process, where the physicochemical characteristics of CdO NPs can be finely tuned, and their functionality can be optimized for targeted applications [28].

With the recent rising demand for eco-friendly nanoparticles synthesis techniques and the imperative need for obtaining novel antimicrobial treatments, this work focuses on synthesizing CdO NPs via the PLAL technique, along with assessing their antibacterial characteristics. Specifically, by examining how the varying laser energies (400, 500, and 600 mJ/pulse) harnessed can influence the size and morphology of the NPs. UV spectrophotometer, XRD, and AFM were systematically utilized to probe the optical and structural changes in the nanomaterial characteristics. Besides that, the antibacterial efficacy of CdO NPs against two bacterial strains (Gram-positive and Gram-negative) was evaluated. By optimizing the synthesis parameters, the research aims to establish a better knowledge of how CdO NPs might be designed for enhanced therapeutic potential in biomedical applications, notably antibacterial treatments.

This study investigates the effect of varying laser energy (400, 500, and 600 mJ) on the synthesis of CdO nanoparticles using pulsed laser ablation in liquid (PLAL). It shows how this energy affects the size and energy gap of the particles. The results showed antibacterial activity against S. aureus and E. coli, with the latter being more sensitive, and the efficacy increased as the laser power increased. The study discusses the mechanisms of action of CdO NPs, such as the generation of reactive oxygen species (ROS) and direct interaction with bacterial membranes, demonstrating their potential in combating antibiotic-resistant bacteria. The study highlights PLAL as a clean and environmentally friendly way to synthesize particles, making CdO NPs a promising option in biomedical applications.

2. Experimental

2.1 CdO NPs synthesis via PLAL

Cadmium oxide (CdO) NPs were prepared via the PLAL technique. In the experiment, a CdO with high purity (99%) was utilized. The NPs were deposited at the base of a glass jar containing 3 mL of DI water, which served as a medium for nanoparticle synthesis, along with a means to control excessive heating of the target. A Q-switched Nd: YAG laser (Model HF-301, Huafei Technology, China) was employed to ablate the CdO target. The laser emitted light at a wavelength of 1064 nm

and was operated at different pulse energies, including 400, 500, and 600 mJ per pulse, to explore the impact of energy variation on the ablation process.

The laser had a pulse frequency of 6 Hz and a pulse duration of 10 ns, which is critical for achieving precise and efficient ablation of the target material. The focal length of the lens used to focus the laser beam onto the target surface was 120 mm. The beam was focused onto a small spot on the target surface, which was submerged in the DI water layer. The depth of the water above the target was approximately 10 mm, which was chosen to optimize the ablation process by minimizing the scattering and absorption of the laser beam by the nanoparticles formed in the water. More details can be found elsewhere [29].

During the laser ablation process, nanoparticles were generated and suspended in the DI water. Since the accumulation of nanoparticles in the liquid can lead to shielding of the laser beam and uneven ablation, the glass vessel containing the CdO target was continuously rotated at a low speed throughout the ablation process. This rotation ensured that fresh areas of the target were constantly exposed to the laser, reducing the likelihood of nanoparticle clustering or the laser beam being blocked by previously formed particles [30]. In total, 200 laser pulses were applied to each sample, ensuring a consistent and repeatable production of nanoparticles at the various energy levels.

The resulting colloidal solution containing the synthesized CdO nanoparticles was visually inspected for color changes, which provided an initial indication of successful nanoparticle formation. Typically, the water shifted from clear to a pale brown, suggesting the presence of suspended nanoparticles Figure 1.

2.2 Preparation of CdO nanoparticle films

To prepare samples for further evaluation, CdO NPs were drop-cast onto glass slides. The colloidal solution was initially concentrated by allowing the water to evaporate somewhat at a regulated temperature of 60 °C. A small amount of concentrated solution was carefully pipetted and dropped onto pre-cleaned glass slides. By using an ultrasonic bath, the slides were carefully cleaned prior to the deposition process. Initially, the slides were soaked in DI water and sonicated for 10 minutes to eliminate any surface impurities. Following washing by ultrasonics, the slides were immersed in methanol for 10 min to ensure that all organic residues were removed and the nanoparticle film adhered properly. Then the cleaned slides were dried in the air before use. Once the CdO NPs solution was deposited onto the glass slides, the samples were placed in an oven at 60 °C for drying. This step is necessary for facilitating the evaporation of the remaining solvent, leaving behind a uniform CdO NPs thin film. This process ensured the formation of well-adhered NPs films on the glass substrate, which were later harnessed for optical and structural characterization [31].

2.3 Antibacterial testing of CdO nanoparticles

The antibacterial efficacy of the synthesized CdO NPs was assessed through two bacterial strains: E. coli (Gram-negative) and S. aureus (Gram-positive). Both strains were cultured in Muller-Hinton (MH) agar medium. For preparing the bacterial cultures, each of the two strains was taken from fresh inoculum and grown overnight in a nutrient broth at 37 °C, aiming to achieve a fresh and sufficient concentration of bacterial culture. For evaluation of the antimicrobial activity of the produced NPs, the CdO NPs films were then added to bacterial cultures that had been grown in Muller-Hinton agar plates. First, bacterial suspensions that were diluted (about 10^9 CFU/mL) were obtained. A certain amount of the CdO NPs solution was introduced to the plates of bacterial colonies, and the plates were incubated for 24 hours at 37 °C. Following the incubation step, the bacterial growth was determined by manual counting of the number of viable colonies on each plate. The obtained results were finally compared to a standardized control plate prepared aside without nanoparticle treatment to detect the capability of the CdO NPs in inhibiting bacterial growth. Finally, by measuring the reduction in colony-forming units (CFU) after treatment with the nanoparticles, bacterial inhibition was determined. This procedure bestows an indication of the minimum inhibitory concentration (MIC) necessary for bacterial inactivation [31].

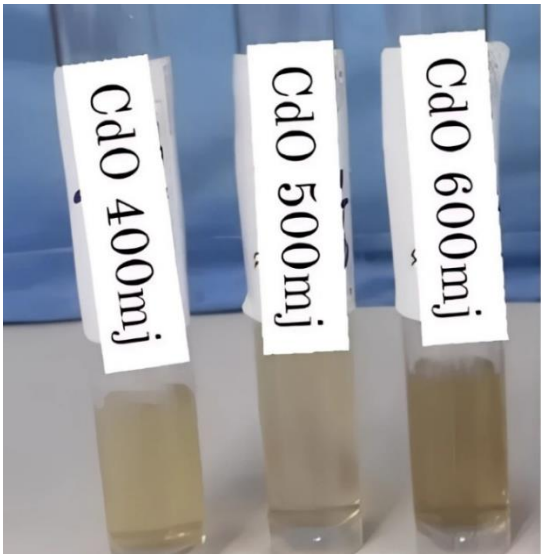

Figure 1: CdO nanoparticles

3. Results and discussion

3.1 Optical properties

The color change of DI water from almost clear to slightly brown by the PLAL process can be considered as a confirmation of the production of CdO NPs. This color change depicts the effective formation of nanoparticles suspended in liquid, which is a common feature of PLAL synthesis.

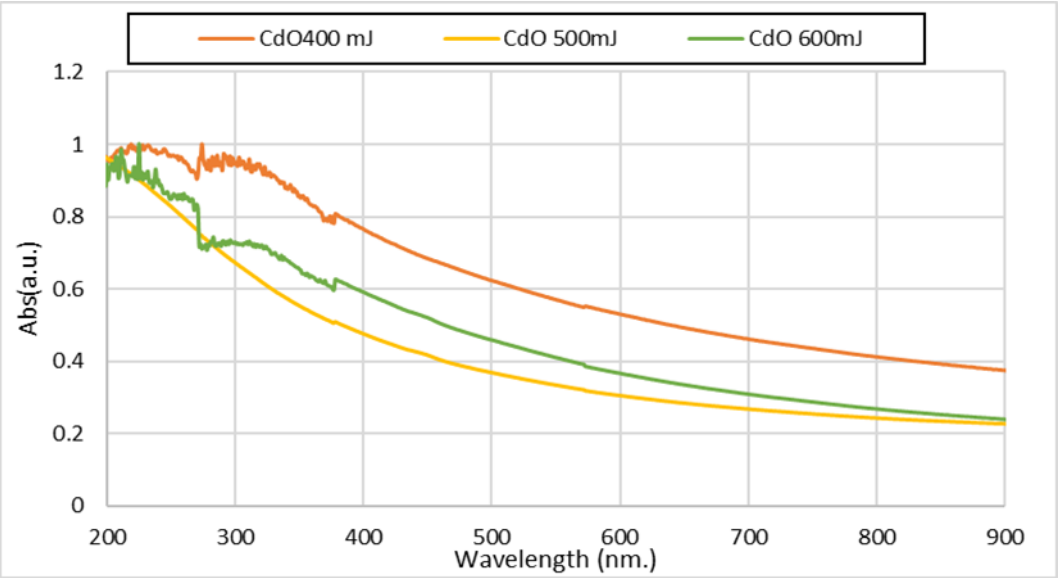

Figure 2: Absorption presented as a function of wavelength

Across the measured laser energy, the CdO NPs exhibit a noticeable absorption peak at 300 nm, according to the UV-Vis absorption spectra displayed in Figure 2. An increase in laser energy induced a greater concentration of ablated nanoparticles, which broadens the absorption spectrum and raises the intensity of absorbance, indeed. A more apparent plasmon resonance results from the creation of more nanoparticles at higher energy, which is the cause of this intensity rise. Increased optical activity as particle concentration increases is the result of the plasmonic effect, which is commonly attributed to MO nanoparticles. The optical bandgap of the CdO NPs was determined through Tauc's rule [22]. For direct electronic transitions, the calculation consisted of several key parameters, as illustrated in Equation 1. These include the optical energy gap (Eg), the absorption coefficient (α), the incident photon energy (hν), and a material-dependent constant (A).

$$(\alpha h\upsilon)^2 = A\,(\,h\upsilon - E_g\,) \quad (1)$$

The bandgap values were found to decrease with increasing laser energy, measured at 2.6 eV, 2.56 eV, and 2.38 eV for laser energies of 400, 500, and 600 mJ, respectively Figure 3. This narrowing of the bandgap with higher laser energy could be ascribed to quantum confinement effects, where a smaller size of nanoparticles can enhance their electronic properties. As the size of the nanoparticles declines, the energy levels become more discrete, leading to a widening of the bandgap. At higher energy levels, the separation between the overlapping s- and p-electron conduction bands becomes more pronounced. This implies that the interactions among these electronic states are more likely to induce a reduction in the bandgap [32].

3.2 Structural properties

3.2.1 XRD Analysis

XRD Analysis provided insights into the crystallographic structure of the CdO NPs synthesized at varying laser energies. As displayed in the Figure 4. The observed diffraction peaks align with the (111), (200), (202), (311), and (222) crystal planes, which are the characteristic of the face-centered cubic (FCC) structure of CdO NPs, as confirmed by JCPDS card No. 05-0640. This observation validates the effective synthesis of CdO NPs with a polycrystalline structure and is in line with earlier studies. The sharpening of the diffraction peaks showed that the CdO NPs' crystallinity improved as the laser energy rose.

Regardless of the laser energy utilized, the lack of impurity peaks in all samples indicates that the produced nanoparticles are very pure. The crystallite sizes determined by the Debye-Scherrer Equation are represented in Table 1. Although larger particle production results from higher ablation rates at higher energies, it is clear that the average crystallite size grows as laser energy increases. This correlation between laser energy and crystallite size is consistent with the results of related research on the creation of nanoparticles [33].

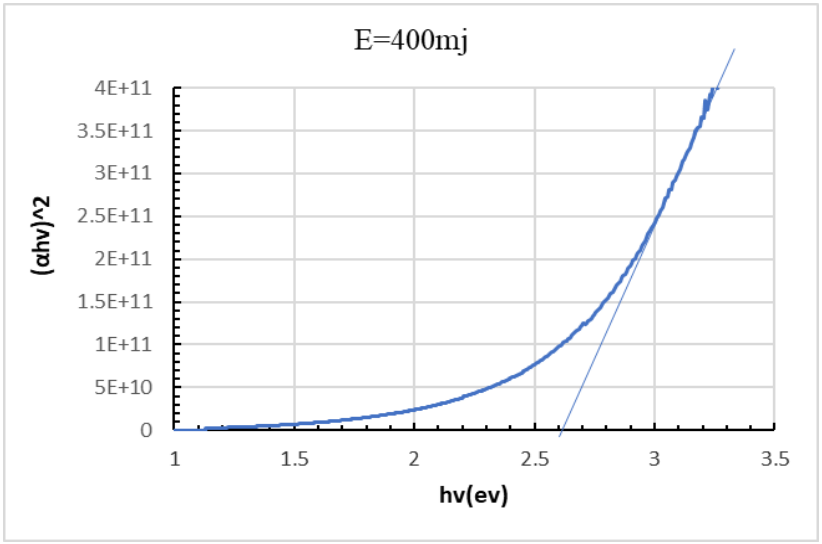

(a)

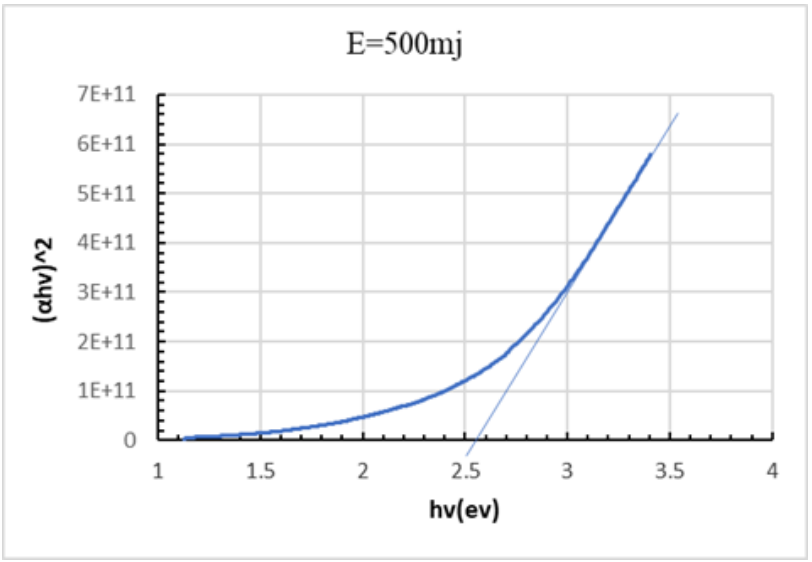

(b)

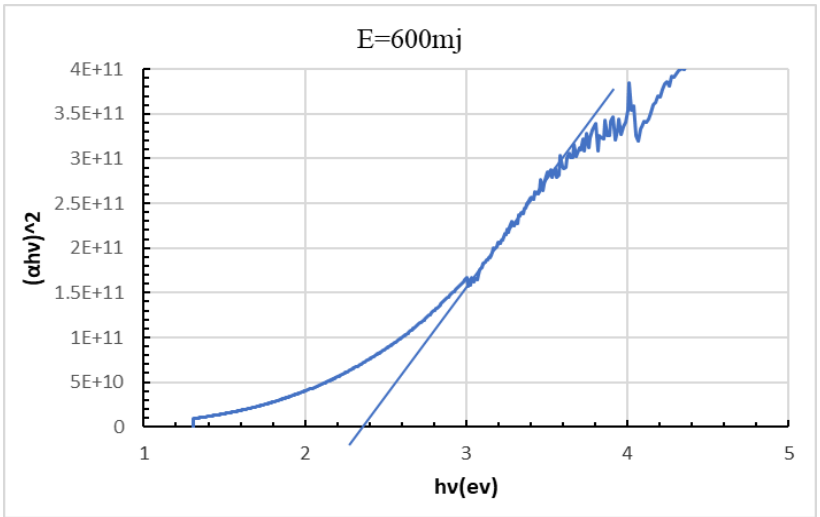

(c)

Figure 3: Energy gap of CdO NPS at different laser energies (a) 400 mJ, (b) 500 mJ, and (c) 600 mJ

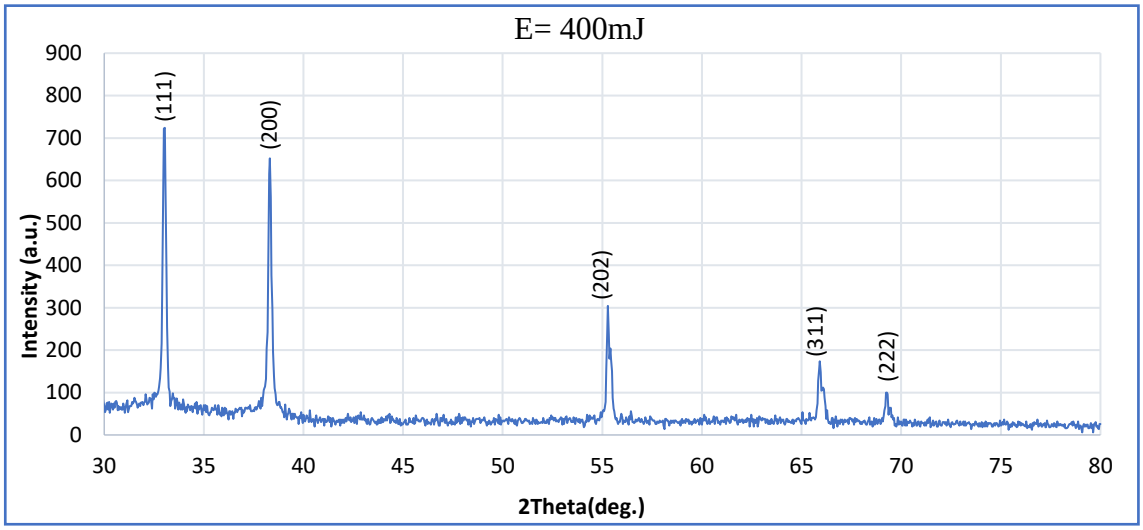

(a)

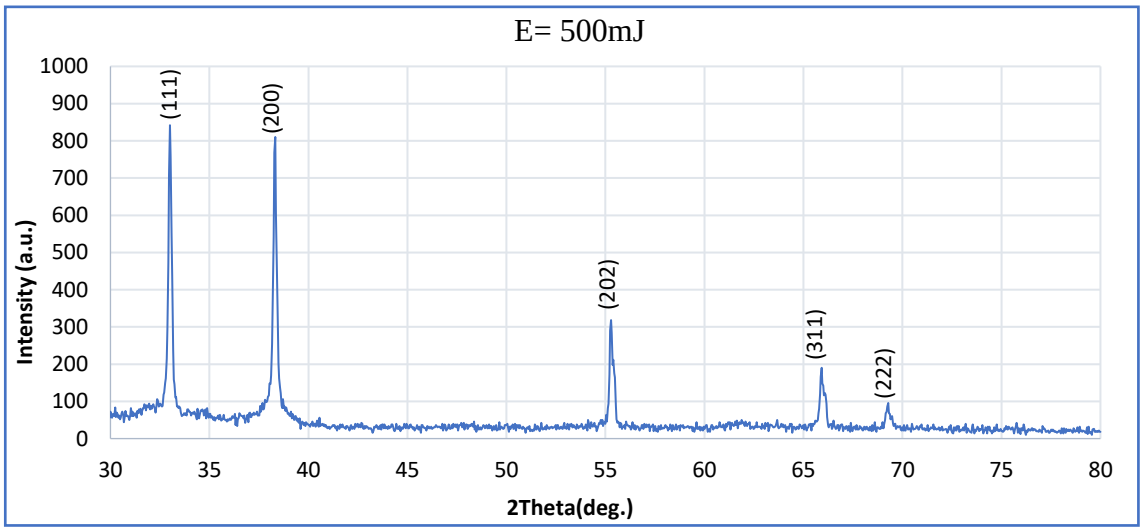

(b)

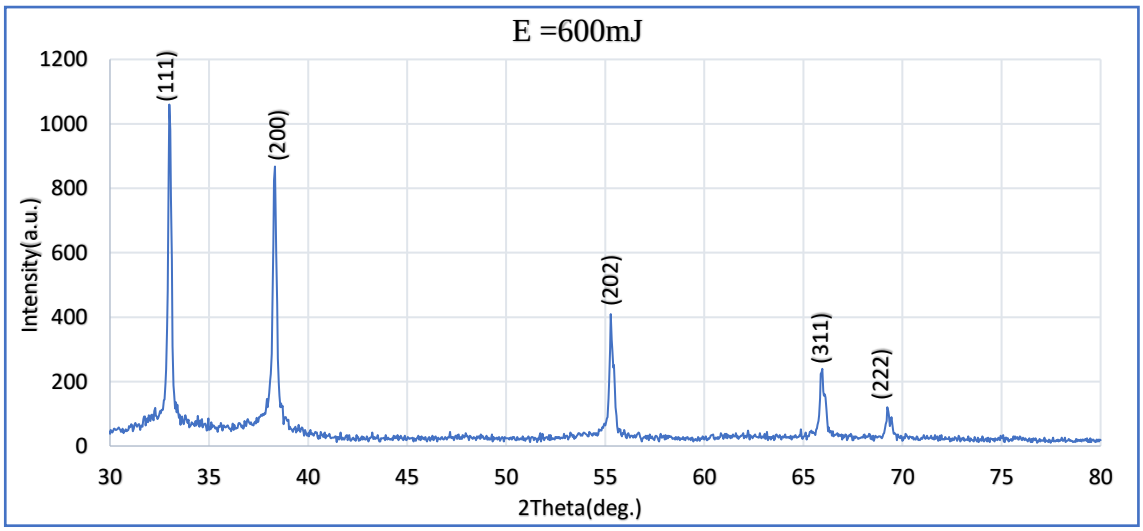

(c)

Figure 4: XRD of CdO Nps at different energy levels (a) 400 mJ, (b) 500 mJ, (c) 600 mJ

Table 1: The CdO NPs crystalline size prepared at various energies

Laser Energy	2Theta (deg.)	FWHM (deg.)	C.S. (mm)	hkl
400mJ	33.04	0.24	34.6097	111
	38.32	0.24	35.12.35	200
	55.28	0.16	56.15.45	202
	65.92	0.24	39.5113	311
	69.28	0.16	60.4336	222
500mJ	33.00	0.24	34.6061	111
	38.32	0.24	35.1235	200
	55.28	0.16	56.1545	202
	65.92	0.24	39.5113	311
	69.24	0.24	40.2794	222
600mJ	33.00	0.16	51.9092	111
	38.32	0.24	35.1235	200
	55.28	0.16	56.1545	202
	65.92	0.32	29.6334	311
	69.24	0.16	60.4336	222

3.2.2 Atomic force microscopy (AFM)

The surface morphology and size distribution of CdO NPs have been examined using AFM analysis. The AFM images of CdO NPs generated at 400, 500, and 600 mJ laser energy are displayed in Figure 5. According to the AFM analysis, average nanoparticle diameters for 400, 500, and 600 mJ were 133.07, 97.79, and 84.26 nm, respectively, indicating that the average nanoparticle size diminishes as laser energy increases. A common characteristic of the PLAL process is the trend of decreasing size as laser energy rises; more laser energy results in more intense ablation and finer particle sizes [31].

In addition to size, the surface roughness of the nanoparticles also decreased with increasing laser energy. Table 2 shows the average roughness values, which were found to decrease from 12 nm at 400 mJ to 6.29 nm at 600 mJ. This reduction in roughness indicates the formation of smoother and more uniform nanoparticles at higher energies, which is desirable for applications where consistent surface characteristics are crucial, such as in antibacterial coatings.

Table 2: The roughness parameters and average diameter of CdO NPs produced using various laser energies

Energy(mJ)	Avg. Diameter (nm)	Root Mean Sq. (nm)	Avg. Roughness (nm)
400	133.07	12	10.4
500	97.79	30.8	26.6
600	84.26	6.29	5.36

3.3 Anti-bacterial effect

The antibacterial efficacy of CdO was evaluated using two strains of E. coli and Staph. aureus bacteria. Results of the antibacterial activity tests are depicted in Figure 6 and given in Table 3 below. The bacterial colonies were counted before and after treatment with CdO nanoparticles at different laser energies. Meanwhile, the results disclosed that CdO nanoparticles manifested significant antibacterial activity against both Staph. Aureus and E. coli. However, the antibacterial activity was shown to be more effective against E. coli, which is consistent with the fact that Gram-negative bacteria are generally more susceptible to nanoparticle penetration due to their thinner peptidoglycan layer. The antibacterial activity increased with increasing laser energy, with the most substantial reduction in bacterial colonies observed at 600 mJ. For E. coli, the colony count reduced from 8×10^9 CFU/mL (before treatment) to 0.39×10^9 CFU/mL, 0.40×10^9 CFU/mL, and 0.79×10^9 CFU/mL for the nanoparticles synthesized at 400, 500, and 600 mJ, respectively. For S. aureus, the colony count reduced to 3×10^9 CFU/mL, 3.9×10^9 CFU/mL, and 4×10^9 CFU/mL for the same energy levels.

The increased surface area and smaller nanoparticle size, which promote better interaction between the nanoparticles and bacterial cells, are undoubtedly the causes of the enhanced antibacterial effectiveness at higher laser energy. CdO NPs likely kill bacteria by generating reactive oxygen species (ROS) and physically interacting with bacterial membranes, leading to their disruption and ultimately causing cell death.

Table 3: The effect of NPs treatment with E. coli and S. aureus

Prior treatment	Following treatment		
$8x10^9$ Colony/ml	**Energy (mJ)**	**E. Coli Colony/ml**	**S. aureus Colony/ml**
	400	$0.39x10^9$	$3x10^9$
	500	$0.4x10^9$	$3.9x10^9$
	600	$0.79x10^9$	$4x10^9$

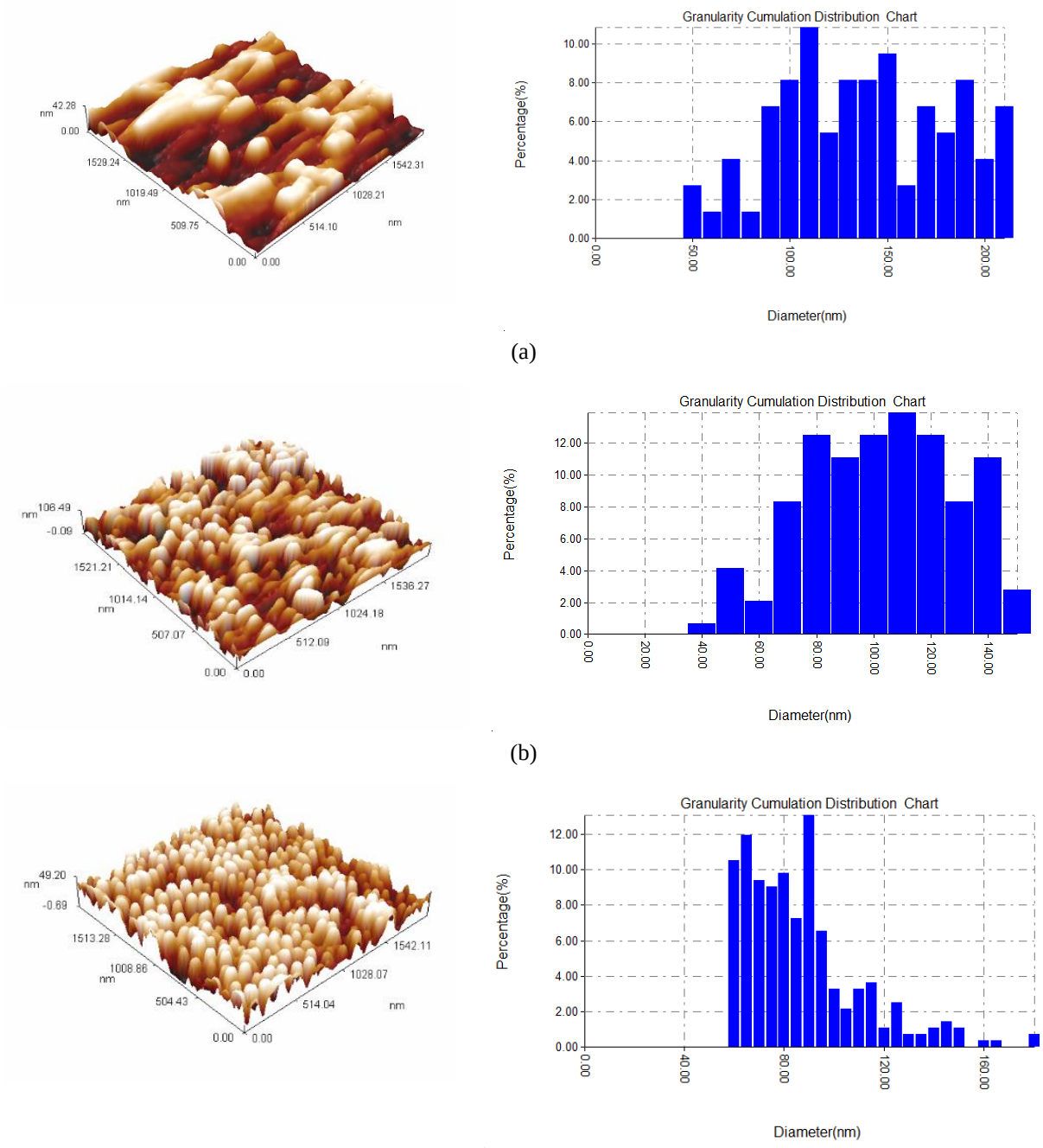

Figure 5: At various laser energy AFM pictures and size distribution of CdO NPs (a) 400 mJ, (b) 500 mJ, (c) 600 mJ

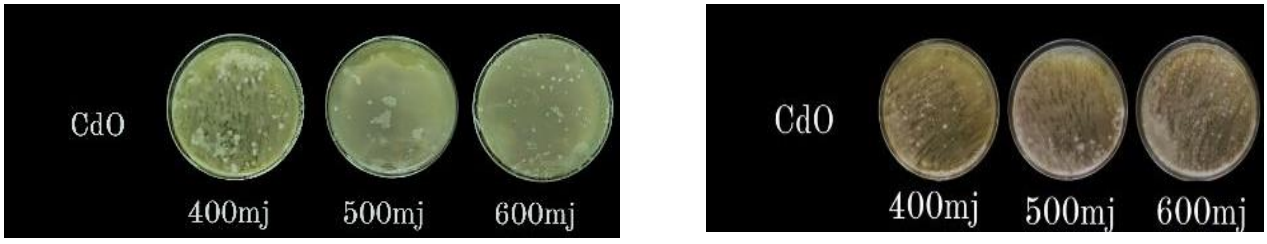

(a) (b)

Figure 6: The bacterial colonies (a) E.Coli ; (b) Staph. Aureus, after treatment by nanoparticles at different energies

4. Conclusion

This study clearly demonstrated how CdO nanoparticles were created using various laser energies. From the XRD characterization, one can see that CdO has the polycrystalline structure of cubic phases, and when the crystal size was raised as a result, the diffraction peaks shrank within the nanometer range, and the peak width was proportional to the nano-crystalline size. AFM analysis revealed that as laser energy increases, the average diameter drops for PLAL thin films. The optical characteristics of the films indicate that a direct transition was possible. This study's nanoparticles show Antibacterial activity against Gram-positive (Staphylococcus aureus) and Gram-negative (Escherichia coli) microorganisms. This method generates nanoparticles having antibacterial capabilities, which might be useful in the development of highly effective agents.

Acknowledgment

The authors would like to thank the University of Mustansiriyah, the University of Baghdad, Baghdad, Iraq, and Al-Balqa Applied University, Amman, Jordan, for their support in completing this work.

Author contributions

Conceptualization, **A. Yousif, T. Mejbel, K. Aadim, and W. Kadhem**; methodology, **A. Yousif**; software, **T. Mejbel,** and **K. Aadim**; validation, **A. Yousif, T. Mejbel, K. Aadim, and W. Kadhem**; formal analysis, **A. Yousif, and T. Mejbel**; investigation, **A. Yousif, T. Mejbel, K. Aadim, and W. Kadhem**; resources, **T. Mejbel, and K. Aadim**; data curation, **A. Yousif**; writing—original draft preparation, **T. Mejbel** and **K. Aadim**; writing—review and editing, **A. Yousif,** and **W. Kadhem**; visualization, **A. Yousif**; supervision, **A. Yousif**; project administration, **A. Yousif**; funding acquisition, **A. Yousif, T. Mejbel, K. Aadim, and W. Kadhem**. All authors have read and agreed to the published version of the manuscript.

Funding

This research received no external funding.

Data availability statement

The data that support the findings of this study are available on request from the corresponding author.

Conflicts of interest

The authors declare no conflicts of interest.

References

[1] A. M. Negrescu, M. S. Killian, S. N. Raghu, P. Schmuki, A. Mazare, A. Cimpean, Metal oxide nanoparticles: review of synthesis, characterization and biological effects, J. Funct. Biomater., 13 (2022) 274. https://doi.org/10.3390/jfb13040274

[2] A. Z. Skheel, M. H. Jaduaa, A. N. Abd, Green synthesis of cadmium oxide nanoparticles for biomedical applications (antibacterial, and anticancer activities), Mater. Today: Proc., 45 (2021) 5793-5799. https://doi.org/10.1016/j.matpr.2021.03.168

[3] M. Bruchez Jr, M. Moronne, P. Gin, S. Weiss, A.P. Alivisatos, Semiconductor nanocrystals as fluorescent biological labels, Sci., 281 (1998) 2013-2016. https://doi.org/10.1126/science.281.5385.2013

[4] C. Mah, I. Zolotukhin, T. Fraites, J. Dobson, C. Batich, B. Byrne, Microsphere-mediated delivery of recombinant AAV vectors in vitro and in vivo, Mol Ther, 1 (2000) S293.

[5] R. A. Edelstein, C. Tamanaha, P. Sheehan, M. Miller, D. Baselt, L. Whitman, R. Colton, The BARC biosensor applied to the detection of biological warfare agents, Biosens. Bioelectron., 14 (2000) 805-813. https://doi.org/10.1016/S0956-5663(99)00054-8

[6] J.-M. Nam, C. S. Thaxton, C. A. Mirkin, Nanoparticle-based bio-bar codes for the ultrasensitive detection of proteins, Sci., 301 (2003) 1884-1886. https://doi.org/10.1126/science.1088755

[7] R. Mahtab, J. P. Rogers, C. J. Murphy, Protein-sized quantum dot luminescence can distinguish between" straight"," bent", and" kinked" oligonucleotides, J. Am. Chem. Soc., 117 (1995) 9099-9100. https://doi.org/10.1021/ja00140a040

[8] J. Ma, H. Wong, L. Kong, K. Peng, Biomimetic processing of nanocrystallite bioactive apatite coating on titanium, Nanotechnol., 14 (2003) 619. https://doi.org/10.1088/0957-4484/14/6/310

[9] M. Shinkai, M. Yanase, M. Suzuki, H. Honda, T. Wakabayashi, J. Yoshida, T. Kobayashi, Intracellular hyperthermia for cancer using magnetite cationic liposomes, J. Magn. Magn. Mater., 194 (1999) 176-184. https://doi.org/10.1016/S0304-8853(98)00586-1

[10] R. S. Molday, D. Mackenzie, Immunospecific ferromagnetic iron-dextran reagents for the labeling and magnetic separation of cells, J. Immunol. Methods, 52 (1982) 353-367. https://doi.org/10.1016/0022-1759(82)90007-2

[11] R. Weissleder, G. Elizondo, J. Wittenberg, C. Rabito, H. Bengele, L. Josephson, Ultrasmall superparamagnetic iron oxide: characterization of a new class of contrast agents for MR imaging, Radiology, 175 (1990) 489-493. https://doi.org/10.1148/radiology.175.2.2326474

[12] A. A. Yousif, M.H. Hasan, Gas sensitivity and morphologically characterized of nanostructure CdO doped In2O3 films deposited by pulsed laser deposition, J. Biosens. Bioelectron., 6 (2015) 1. http://dx.doi.org/10.4172/2155-6210.1000192

[13] H. R. Abed, A. I. Khudadad, A. A. Yousif, Impact of high vacuum annealing temperature on the structural, photoluminescence, and room temperature liquefied petroleum gas sensing of direct current magnetron sputtered CdO films, Mater. Chem. Phys., 289 (2022) 126446. https://doi.org/10.1016/j.matchemphys.2022.126446

[14] Ö. Güler, Ö. Başgöz, M. G. Albayrak, M. Takgün, The Properties of Cadmium Oxide-Carbon Nanotube Nanocomposite Synthesized Via Sol-Gel Method, Eur. J. Tech., 9 (2019) 25-36.

[15] J. C. Rhoda, S. Chellammal, H. M. Albert, K. Ravichandran, C.A. Gonsago, Synthesis, spectroscopic, and antibacterial characterizations of cadmium–based nanoparticles, J. Fluoresc., 34 (2024) 587-598.

[16] A. W. Metz, J. R. Ireland, J.-G. Zheng, R. P. Lobo, Y. Yang, J. Ni, C. L. Stern, V. P. Dravid, N. Bontemps, C. R. Kannewurf, Transparent conducting oxides: texture and microstructure effects on charge carrier mobility in MOCVD-derived CdO thin films grown with a thermally stable, low-melting precursor, J. Am. Chem. Soc., 126 (2004) 8477-8492. https://doi.org/10.1021/ja039232z

[17] M. P. Nikolova, M. S. Chavali, Metal oxide nanoparticles as biomedical materials, Biomimetics, 5 (2020) 27. https://doi.org/10.3390/biomimetics5020027

[18] A. Dixit, R. Bala, B. Pareek, A. Chaudhary, V. S. Jaswal, A review on synthesis of Cadmium and Manganese oxide nanoparticles with its vitro applications, J. Univ. Shanghai Sci. Technol., 23 (2021).

[19] S. T. Hossain, S. K. Mukherjee, CdO nanoparticle toxicity on growth, morphology, and cell division in Escherichia coli, Langmuir, 28 (2012) 16614-16622. https://doi.org/10.1021/la302872y

[20] M. Shukla, S. Kumari, S. Shukla, R. Shukla, Potent antibacterial activity of nano CdO synthesized via microemulsion scheme, J. Mater. Environ. Sci, 3 (2012) 678-685.

[21] A. N. Abd, M. F. Al Marjani, Z. A. Kadham, Synthesis of CdO NPs for antimicrobial activity, Int. J. Thin Films Sci. Technol., 7 (2018) 43-47.

[22] K. Velsankar, S. Sudhahar, G. Maheshwaran, M. Krishna Kumar, Effect of biosynthesis of ZnO nanoparticles via Cucurbita seed extract on Culex tritaeniorhynchus mosquito larvae with its biological applications, J. Photochem. Photobiol., B, 200 (2019) 111650. https://doi.org/10.1016/j.jphotobiol.2019.111650

[23] J. Rhoda, S. Christina, Chellammal, Helen Merina Albert, K. Ravichandran, and C. Alosious Gonsago, Synthesis, Spectroscopic, and Antibacterial Characterizations of Cadmium-Based Nanoparticles, J. Fluoresc., 34 (2024) 587-598. https://doi.org/10.1007/s10895-023-03290-4

[24] O. A. Fahad, Structural, morphological, and antibacterial for cadmium oxide nanoparticles prepared via pulsed laser ablation, J. Opt., (2024). https://doi.org/10.1007/s12596-024-02198-x

[25] N. F. Khdr, B. G. Rasheed, B. M. Ahmed, Review on nanomaterials properties produced by laser technique, IOP Conf. Ser. Mater. Sci. Eng., IOP Publishing, (2021) 012154. https://doi.org/10.1088/1757-899X/1094/1/012154

[26] A. M. El-Khawaga, A. Zidan, A. I. Abd El-Mageed, Preparation methods of different nanomaterials for various potential applications: A review, J. Mol. Struct., 1281 (2023) 135148. https://doi.org/10.1016/j.molstruc.2023.135148

[27] A. H. Rather, T. U. Wani, R. S. Khan, A. Abdal-hay, S.-u. Rather, J. Macossay, F. A. Sheikh, Recent progress in the green fabrication of cadmium sulfide and cadmium oxide nanoparticles: Synthesis, antimicrobial and cytotoxic studies, Mater. Sci. Eng.,: B, 286 (2022) 116022. http://dx.doi.org/10.1016/j.mseb.2022.116022

[28] E. El Agammy, M. Hasaneen, A. A. Essawy, S. M. Moustafa, G. Khalil, A. Nassar, Effect of Nd: YAG pulsed laser on the antibacterial activity and physical properties of newly synthesized composites, CdO/Co_3O_4 and Ag/CdO/Co_3O_4, Phys. Scr., 99 (2023) 015903. https://doi.org/10.1088/1402-4896/ad0fca

[29] H. Zeng, X. W. Du, S. C. Singh, S. A. Kulinich, S. Yang, J. He, W. Cai, Nanomaterials via laser ablation/irradiation in liquid: a review, Adv. Funct. Mater., 22 (2012) 1333-1353. https://doi.org/10.1002/adfm.201102295

[30] G. Yang, Laser ablation in liquids: Applications in the synthesis of nanocrystals, Prog. Mater Sci., 52 (2007) 648-698. https://doi.org/10.1016/j.pmatsci.2006.10.016

[31] R. H. Shukur, S. M. Hasan, Cadmium Oxide Nanoparticles Synthesis Using Pulsed Laser Ablation in a Liquid Medium and Investigation of their Antibacterial Activity, Front. biomed. Technol., (2024).

[32] S. Dugan, M. M. Koç, B. Coşkun, Structural, electrical and optical characterization of Mn doped CdO photodiodes, J. Mol. Struct., 1202 (2020) 127235. https://doi.org/10.1016/j.molstruc.2019.127235

[33] K. Aadim, A. Mohammad, M. Abduljabbar, Influence of laser energy on synthesizes of CdO/Nps in liquid environment, IOP Conference Series, Mater. Sci. Eng., IOP Publishing, (2018) 012028. https://doi.org/10.1088/1757-899X/454/1/012028